***Proceedings of the IASS 2024 Symposium***
*Redefining the Art of Structural Design*
August 26-30, 2024, Zurich Switzerland
Philippe Block, Giulia Boller, Catherine DeWolf,
Jacqueline Pauli, Walter Kaufmann (eds.)

# Walking on eggshells: innovative methods to justify reuse of a historic thin shell roof at Smithfield Poultry Market

Guusje UBACHS[a,*], Christopher NOBLE[a], Balduino DEL PRINCIPE[a], Richard LAWSON[a]

[a, *] Arup, 8 Fitzroy Street, London W1T 4BJ, United Kingdom
guusje.ubachs@arup.com

## Abstract

This paper describes the pioneering original design and construction of the 1960s historic concrete shell structure of the Smithfield Poultry Market Roof in London, and the sophisticated and innovative method used to breathe new life into this unique structure. This method combines a first order reliability approach with an advanced digital workflow that enabled a detailed technical analysis of the as-built structure. This method demonstrated the structure can meet the modern-day performance requirements without the need for any strengthening works – the most sustainable outcome which allows this beautiful structure to continue its legacy.

**Keywords**: Concrete shell, historic structure, thin shell, refurbishment, reuse, digital workflow, reliability, 20th century concrete shell, sustainability.

## 1. Original structure and design

The 20th century saw many concrete shells built, popular for their efficiency and structural beauty. Many of these unique structures have been lost over time, but there is great potential for reusing those still in existence.

London's Smithfield Poultry Market roof presents an example of how concrete shells can be reimagined through a change of use of the large space they enable, and the challenges of doing so. It is a doubly-curved elliptical paraboloid concrete shell spanning approximately 70m by 40m, with a design thickness of 76mm – only 1/13th of the thickness of an eggshell when compared to its relative span. Constructed in the 1960s, this shell was at the forefront of engineering as one of the largest of its kind.


Figure 1 – Smithfield poultry market exterior (left) and interior (right) © Historic England Archive

### 1.1 Design

The Smithfield Poultry Market roof in London was designed by T. P. Bennett and Son and Arup in the 1960s to replace the original market roof that had been lost to a fire. To span the 70m by 40m market hall, they chose to build a doubly-curved elliptical paraboloid concrete shell. This shape gives a good

curvature and is mathematically well defined, resulting in an efficient, economical, and aesthetically pleasing shape. For the rise of the shell, conventional span to rise ratios at the time would have required a rise of 15m, however, structural engineers Ahm and Perry [1] wrote at the time that the rise had to be kept to an absolute minimum, although the exact reason is not known. Preliminary calculations considering maximum stresses and buckling loading suggested a shallow dome with a rise of 9m would work, although this was less than any shell built at the time. The thickness of the shell was designed to be only 76mm (3 inches). The concrete shell contains four layers of orthogonal rebar (top and bottom, in two directions) as well as a single layer of diagonal rebar at the centre of the concrete. In the corners, the diagonal reinforcement increases in size and density to withstand the greater diagonal tension forces across the corners. The roof edge beams and roof overhangs are supported on V-columns along the perimeter (Figure 2).

Preliminary design was done by membrane theory, using differential equations and published tables to aid the design. The ratio of the rises in the two spanning directions was chosen to be 1:2 to even out the maximum stresses in the surface and producing a pleasing shape [1]. Detailed analysis was carried out using bending theory and working stresses. The effect of edge moments was significant – at the edge of the roof the membrane theory assumptions start to break down, and large moments are generated. This is especially true for shallow domes, and these moments required the edge of the dome to be thickened. The edge was thickened from 76mm to 158mm over a length of 3.5m (Figure 2), based on an approximate analysis of an equivalent singly-curved cylindrical shell.

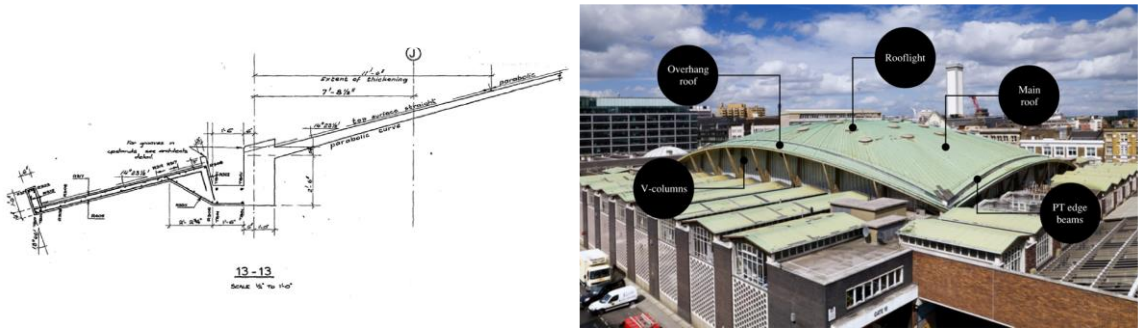


Figure 2 – Section through roof edge and overhang (from archive drawings) (left) and roof exterior (right)

Load on a doubly-curved shell will generate a shearing force along its edge, resulting in a tension along the edge beam supporting the shell. This creates an incompatibility with the membrane forces which was counteracted by post-tensioning the edge beams. This post tensioning would also help lift the shell of its formwork in the construction stage.

### *1.1.2 Snap through buckling*

It was understood at the time that second-order snap through buckling was critical for the design of the shell. A shallow concrete shell is particularly sensitive to this failure mode, which would result in a global failure and collapse of the roof. The applied uniformly distributed load across the roof that the structure can resist against snap through, the critical load $F_{cr}$, was determined using the following equation:

$$F_{cr} = CE \cdot t^2 / R_1 R_2 \quad [kPa] \tag{1}$$

Where t is the thickness of the concrete shell, $R_1$ and $R_2$ are the principal radii of curvature, E is the Young's Modulus of the concrete, and C is a constant to be determined experimentally.

To work out this constant, a model test was carried out at a scale of 1:12. The model shell was 6mm thick, made from cement and sand, and reinforced with 1mm diameter wire. Loading was applied by air bags on the top of the shell in symmetric and asymmetric combinations, and over 80,000 measurements of strain and deflection were taken. The results were processed with a purpose built programme on an early computer, which was estimated at the time to only cost 1/6$^{th}$ of the amount it would have taken to compute the results by hand [2] – a true early example of a digital workflow.

The model test confirmed that the failure mode of the structure was snap through buckling, see Figure 3. The results from the test were in "reasonable agreement" [1] with those from the detailed bending theory calculations. The final design of the shell was therefore completed based on the bending theory. Additionally, during test the edge beams showed signs of cracking under the design load, therefore it was decided to increase the prestressing in these by 40% to avoid failure in the edge beams [1].

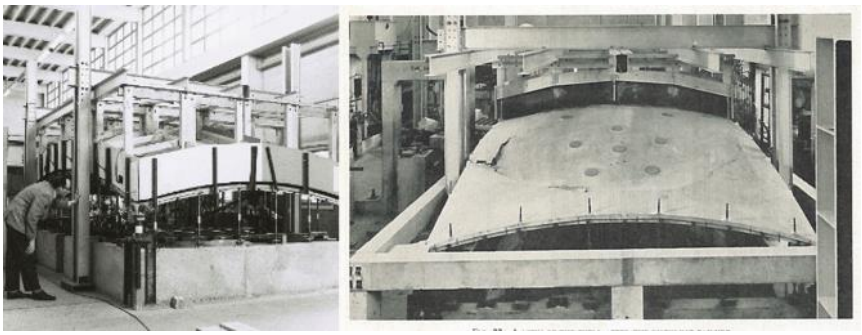

Figure 3 – Model testing (left) and snap through buckling failure (right) © Sydney W Newbery

### 1.2 Construction

The building was constructed in the early sixties by Sir Robert McAlpine. The columns and edge beams were constructed first, and a small amount of post-tensioning was applied to the edge beams. The formwork for the roof shell consisted of singly-curved plywood panels, which were faceted in one direction to achieve the doubly-curved shape. The roof was cast in sequence, working from the corners towards the middle of the roof. A series of openings and upstands for rooflights were cast into the structure in this process as well.

Once the shell was cast, the edge beams were prestressed in a symmetrical sequence. A sliding detail at the corner columns during the construction stage allowed the roof to lift off the formwork during the post-tensioning. Once this was complete, the finishes build-up was laid on the roof, completed with the now iconic copper finish on the top. The market was opened in May 1963, and was reported to be the largest concrete shell of its type at the time by [3].

Figure 4 – Construction of the market roof in the 1960s © John Maltby

## 2. Present day – Restoration and reuse

60 Years later, with the original design life of the structure exceeded, the challenge was to develop a strategy to justify the re-use of the roof. The structure is due to become part of the future Museum of London, a change of use from its original purpose of a meat market. Arup was appointed by Equans, the contractor appointed by the City of London to carry out these enabling works. The design team was posed the challenge of justifying the roof according to the performance criteria established by the modern standards to allow its continuing use. This includes a new build-up of roof finishes with enhanced insulation to improve the energy efficiency of the building, as well as a new layer of copper on top. Underneath the new insulation will be a layer of levelling screed to provide an even surface for the insulation to bear onto. This build-up of finishes was specified to weigh no more than the original build-up, i.e. 'no worse than existing'.

Several considerations went into justifying the re-use of this structure. It was not possible to simply state that because the structure had already existed for 60 years, it would be sufficient to carry a new finishes build-up that was 'no worse than existing'. 'No worse than existing' relies on the acceptance of the existing risk of the structure. But what is the existing risk, and how is it quantified? Secondly, the unloading (removing the original finishes) and the reloading (placing the new finishes) sequence would have to be considered carefully and investigated to assess the impact on this sensitive structure.

Due to these considerations, and the uniqueness of this structure, a detailed assessment was required, including material testing of the concrete, and an investigative survey of the as-built shape of the roof structure.

## 3. Assessing the original structure

### 3.1 Material testing

Material testing was carried out to determine the properties of the concrete in comparison with the design intent from the 1960s. The number of batches and core samples were limited to avoid excessive damage to the existing structure while obtaining a suitable number for a statistical assessment. The test results showed that the concrete compressive strength (and subsequently the tensile strength) and the Young's Modulus were significantly lower than the design intent, see Table 1.

Table 1 – Concrete Properties – Design intent vs test results

| | Design intent | Test result |
|---|---|---|
| Concrete compressive strength, $f_{ck}$ (characteristic) | 34.4 Mpa | 26.3 Mpa |
| Concrete tensile strength, $f_{ctm}$ (mean) | 3.2 Mpa | 2.6 Mpa |
| Young's Modulus, E (characteristic) | 36.5 Gpa | 18.0 Gpa |

Condition surveys were also carried out to establish that the shell was generally in good condition, however more significant repairs were needed to the supporting structure (such as the V-Columns) as part of the enabling works for the building.

### 3.2 Geometry survey

The scale of the challenge was further heightened when the results of point-cloud surveys of the top and bottom roof surface were analysed. A comparison between the point cloud surveys and the design intent was undertaken using Rhino and Grasshopper to assess the deviation of the as-built shape of the roof from the intended design. To undertake this comparison, the theoretical design intent surface was plotted in Rhino and overlaid on the surveyed bottom surface of the roof. The resulting vertical differences between the two surfaces are plotted in Figure 5.

This analysis shows that there is a global out-of-tolerance of the current shape compared with the design intent. The construction tolerance specified in the original design is 6.35mm (1/4 inches) in level, and a maximum rate of change of tolerance of 3.2mm in 3m (1/8 inches in 10 feet) [1]. Whilst the surveyed surface includes the movements which have occurred since construction (including creep), the deviations that can be observed in Figure 5 significantly exceed the intended tolerance and expected displacements.

Notably, the roof also shows a significant asymmetrical deviation (or tilt) across its extent, as well as a larger deviation in the corners on the left-hand side of the roof, showing two sizeable depressions in the shell. The observed deviations have a significant implication on the overall structural performance of the roof as the design is heavily dependent on the intended shape.

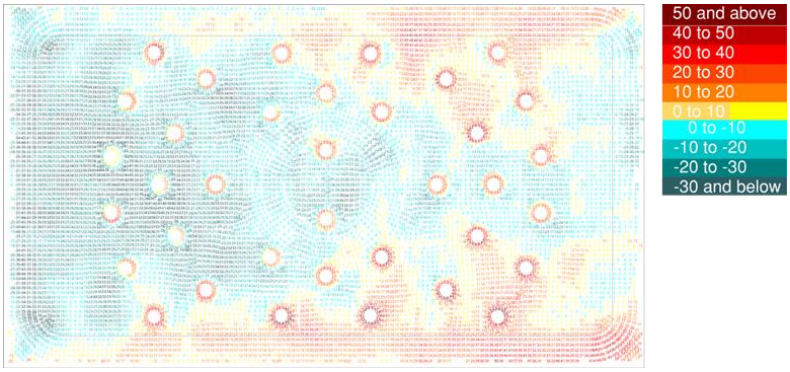


Figure 5 – Relative as-built deviation in mm (as surveyed) from design intent

The roof thickness was also analysed from the survey data. This analysis, shown in Figure 6 below, shows a deviation of the roof thickness with respect to the original design intent drawings. The thickness specified in the archive drawings for the main area of the roof, i.e. the whole shell excluding the thickening around the edges and rooflight openings, is 76mm (3 inches), whereas the survey analysis shows a mean thickness in this area equal to only 73mm, with some locations less than 60mm. Figure 6 shows the distribution of these thicknesses.

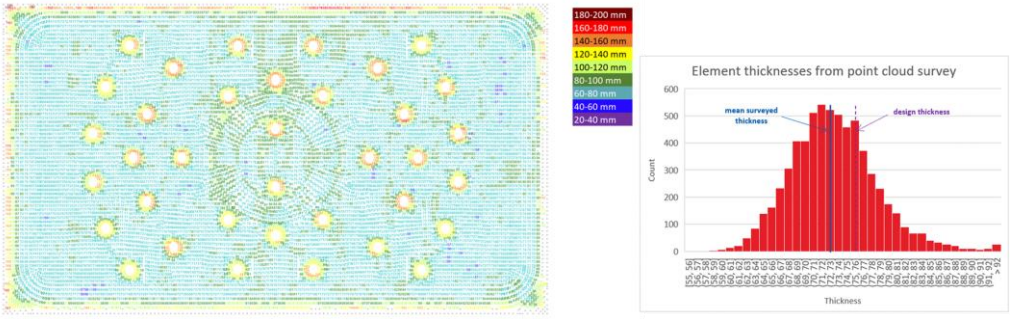


Figure 6 – As-built thickness distribution across the roof in mm (as surveyed)

The combination of the reduced concrete strength and stiffness, smaller roof thickness and the out-of-shape geometry have a substantial impact on the intended capacity of the structure, thus demonstrating that a simple ‘no worse than existing’ approach was not suitable.

## 4. Analysis

Using the survey results, an analysis model was set up in Oasys GSA reflecting the as-built position, including the surveyed geometry, thickness, and material properties. The model was generated from the point cloud survey data using a Grasshopper workflow in Rhino. This also allowed for an accurate assessment of the superimposed dead load of the levelling screed, which is part of the proposed new finishes build-up on the roof. The thickness of this levelling screed varies with the as-built thickness of the roof (Figure 6), therefore the loading from this levelling screed was calculated accurately at each 0.5m centre to incorporate these varying thicknesses.

A detailed conventional analysis to the modern Eurocode standards for new structures was carried out to assess the behaviour of the structure. While the team was able to justify the structure for strength, the snap through buckling analysis showed that for the full Eurocode design loads, the structure fails due to the loss of the stiffness related to the cracking pattern generated by the applied loading on the shell (Figure 7).

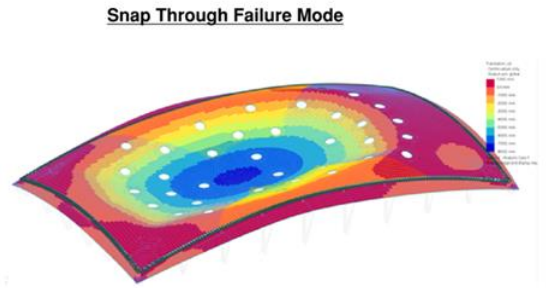


Figure 7 – Snap-through buckling failure in analysis model

This led the design team to take a vastly different approach. To justify the structure, the team approached the challenge from two directions: firstly to determine what a minimum set of acceptable safety factors would be for such an existing structure, and secondly to develop an innovative analysis method, designing out conservatisms and assumptions to refine the assessed capacity of the structure.

### 4.1 Reliability and safety factors: setting the target

The structure was designed in the 1960s according to British Standards of the time. It is important to note that these Standards use a different method – 'working stress' – to check the safety of the structure with respect to that which is prescribed in the current Eurocodes – 'limit state'. Limit state design differs significantly from earlier working stress approaches and has a more developed and accurate scientific basis. Additionally, due to the beneficial effect of post tensioning, the limit state approach gives a more onerous result than the working stress approach.

#### *4.1.1 Reliability index*

As described above, the initial analysis was unable to justify the structure to the conventional Eurocode recommendations for new structures. Because of this, it was deemed more appropriate to assess the reliability index of the roof structure instead. The reliability is defined in the Eurocode as "the ability of a structure or a structural member to fulfil the specified requirements, including the design working life, for which it has been designed [4]". The measure of reliability in the Eurocode is known as the reliability index, $\beta$. This index represents a notional probability of failure based on well-established approximations and is considered sufficiently accurate for structural applications. A higher reliability index implies a lower assessed probability of failure.

The roof structure, which will cover a museum in the future, is deemed to be a Consequence Class 3 (CC3) structure [5]. In designing a new structure to the Eurocodes, a target reliability index of $\beta = 4.3$ is recommended for a CC3 structure [6]. Lower target reliability factors may be used for existing structures. The *fib* indicates that lower values may be more appropriate depending on the consequences of failure and the cost of safety measures [7]. Additionally, Vrouwenvelder and Scholten [8] propose recommended minimum values for life safety for existing structures where strengthening works are deemed not practical or too expensive, for each consequence class.

Together, the *fib* [7] and Vrouwenvelder and Scholten [8] state that a target reliability index of $\beta = 3.3$ may be used for the concrete roof of the Smithfield Poultry Market. Starting from this new reliability index target, the loading partial factors for the load combination could then be derived in accordance with the *fib* Bulletin 80 [7], for which the structure should be justified.

In defining the loading partial factors, the coefficient of variation for self-weight and superimposed dead loads was reduced as a result of the survey carried out. For the self-weight, the coefficient was reduced because the point cloud survey reduces uncertainty about shape and thickness of the roof. For the superimposed dead load, enhanced quality control was put in place on site to ensure that the actual finishes weights were within the loading assumptions.

Based on a reliability index of $\beta$ = 3.3, the following load combination was determined against which the snap through analysis could be undertaken:

$$1.11\,SW\ +\ 0.90\,PT\ +\ 1.18\,SDL\ +\ 1.42\,LL \tag{2}$$

Where SW is the self-weight, PT is the effect from post-tensioning, SDL is the superimposed dead load, and LL is the live load. The live load was taken as a worst-case scenario of a combination of climatic loads, with snow loading as the leading action, and wind loading as the accompanying action.

An assessment was undertaken to reduce the material partial factors in line with the approach outlined above, however these were found to not influence the snap through behaviour of the structure.

### 4.2 Refining the assessed capacity: designing out conservatisms

With this new reliability index target in mind, the next step was to undertake a much more detailed analysis that reduced conservatism and assumptions, to verify the global stability of the structure against snap through failure.

The stiffness and shape of the roof are two of the most important factors in the snap through analysis and must be considered as precisely as possible to enable the verification of the structure. The finite element analysis (FEA) model uses the as-built surveyed shape from the point cloud survey to allow for accurate representation of the geometry and thickness of the structure. The structure in its as-built shape has already experienced the effects of self-weight and post-tensioning, therefore an adjusted 'starting shape' – a geometry that deflects into the as-built position under self-weight and post-tension loading – was found using an iterative workflow hosted in Python. This starting shape is different for each unique set of partial safety factors considered.

#### *4.2.1 Loss of stiffness due to cracking*

Accurately assessing the loss of stiffness due to cracking generated by the applied loading was crucial. The loss of in-plane stiffness from cracking due to tension, the loss of out-of-plane stiffness from cracking due to bending, as well as the effect of twisting moments were all assessed in the analysis. Both in-plane and out-of-plane stiffnesses were assessed in two directions to represent the orthotropic behaviour of the reinforced concrete.

The loading on the roof generates a load path of principal compression into the four corners, and principal tension diagonally across the corners. The typical orthogonal rebar in the roof is generally at a 45° angle from these principal stresses. To assess all these properties in their respective directions independently, the FEA model was set up with a parallel double layer of over 22,000 orthotropic 2D shell elements, connected at their corner nodes. Each pair of shell elements enables independent manipulation of two unique in-plane stiffnesses ($EA_x$ and $EA_y$ in kN) in one 'in-plane' element with axes in the direction of principal stresses in the corners, and two out-of-plane stiffnesses ($EI_x$ and $EI_y$ in $kNm^2$) in the other 'out-of-plane' element with axes in the direction of the orthogonal rebar, see Figure 8. Additionally, the in-plane elements have 0% modifiers applied to out-of-plane stiffness, and the out-of-plane elements have 0% modifiers on the in-plane stiffness, shear stiffness and density. This allowed for precise manipulation of these four stiffnesses per element pair, which meant less conservatism in assessing the loss of stiffness due to cracking.

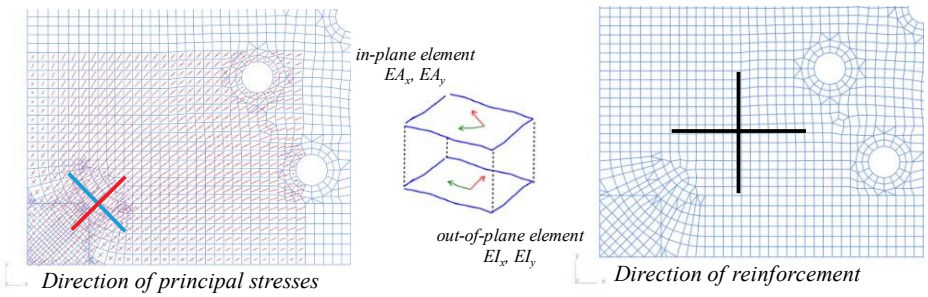


Figure 8 – FEA model set-up and axes conventions

### *4.2.2 In-plane stiffness reductions*

To determine the cracked in-plane stiffness in the elements, the tangent in-plane stiffness with strain offsets were used instead of the more commonly used secant stiffness. When using the force-strain (F-ε) curves to determine in-plane stiffnesses, a secant stiffness may result in negative values which can result in errors in the FEA program. To assess the correct stiffness, the F-ε curve is drawn for the specific bending moment that the element pair experiences. The tangent slope to this curve at the point of the axial force in the element is then used in combination with a strain offset. This strain offset can be found at the intersection of the tangent with the x-axis (strain), see Figure 9. This initial strain is then applied to the FEA in-plane shell element as a pre-strain in combination with the slope of the curve to represent the correct in-plane stiffness, i.e. $EA_x$ with $\varepsilon_x$ and $EA_y$ with $\varepsilon_y$ represent the in-plane stiffness in the element local x and y directions, respectively.

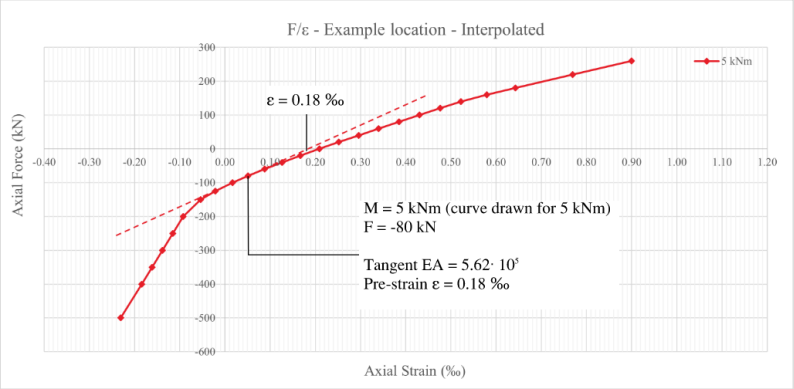


Figure 9 – Example calculation of in-plane stiffness from F-ε graph with a 5kNm moment in the element

### *4.2.3 Out-of-plane and twisting stiffness reductions*

The bending moments used for determining the out-of-plane stiffness reductions in the two directions are:

$$M_x + sign(M_x) \cdot \min\left(|M_x|, |M_{xy}|\right) \; [kNm] \tag{3}$$

$$M_y + sign(M_y) \cdot \min\left(|M_y|, |M_{xy}|\right) \; [kNm] \tag{4}$$

In the FEA 2D shell elements, the principal bending moments are generally not aligned with the reinforcement axes in the element, resulting in a twisting moment $M_{xy}$ [kNm], which is resisted by a diagonal compression in the concrete and tension in the reinforcement. From sensitivity studies, it was found that the twisting moment and the twisting stiffness, had a significant effect on the structural behaviour of the roof.

A calculation was undertaken to convert the applied bending and twisting moments into equivalent bending moments in the two reinforcement directions. From the equivalent moments, bending curvatures were calculated using moment-curvature relationships obtained from the section analysis software (Oasys AdSec), and a consistent twisting curvature was determined. The out-of-plane and twisting stiffnesses ($EI_x$, $EI_y$, $EI_{xy}$) were then obtained by dividing the applied moments by these curvatures. The twisting stiffness parameter $G_{xy}$ was then calculated as:

$$G_{xy} = \frac{EI_{xy}}{2(1+\nu_{xy})I_{xy}} \; [GPa] \tag{5}$$

Where Poisson's ratio $\nu_{xy} = 0$ when an element is cracked in either direction.

### *4.2.4 Digital workflow*

When the stiffnesses in the shell elements across the roof change, the cracking pattern due to the applied loading changes, leading to a new set of stiffnesses for the FEA elements. To find a compatible set of stiffnesses representing the behaviour of the roof, a digital iterative workflow was created to run the analysis, which updates the stiffnesses each iteration. The iterations do not reflect a time-history but they are numerical iterations to find a solution with compatible stiffnesses across the roof.

In each iteration, stresses from the two elements in each element pair are combined and rotated into the in-plane and out-of-plane element respective local axes using Mohr's circle logic, from which the principal stresses can be calculated.

When the combined principal tension of the element pair in the in-plane local axes is greater than the mean concrete tensile strength of 2.6Mpa, the element is deemed as 'cracked in-plane'. An element is deemed as 'cracked out-of-plane' when the combined top or bottom principal tension in the out-of-plane local axes is higher than 2.6 Mpa. This means that out-of-plane actions (bending) have an effect on in-plane stiffnesses, and vice-versa. In each iteration, every shell element is assessed to be 'cracked' or 'not cracked' in its local x and y axes, and is subsequently assigned an updated set of in-plane stiffnesses and out-of-plane stiffnesses ($EA_x$ with $\varepsilon_x$, $EA_y$ with $\varepsilon_x$, $EI_x$, $EI_y$), shear moduli ($G_x$, $G_y$), and twisting stiffness (from $G_{xy}$). Additionally, when an element is cracked its Poisson's ratio $v_{xy}$ is set to 0.

The FEA model is run using Oasys GSA software and the workflow which assesses the stiffnesses as outlined above is hosted in an excel spreadsheet using results from GSA. The exchange of data between the two programs and the running of the workflow is controlled by a VBA script built into the spreadsheet. The spreadsheet also hosts a database of force-strain curves and bending moment-stiffness curves for determining the stiffnesses. Finally, the VBA script produces data and diagrams of the model behaviour at every iteration step, allowing the team to investigate the analysis at each iteration while it is running. This avoids the process being a 'black box' and creates a transparent digital workflow that is easy to interrogate.

This iterative process is run until a converged solution is reached where the changes in stiffness and model behaviour (e.g. deflections) have stabilised. To aid the convergence of the process, the rate of change of stiffness in every iteration is limited, i.e. the stiffness of an element reduces or increases in limited steps. The change in stiffness is limited to a 30% change at the start of the iterative process and is incrementally reduced to 3% stiffness change when the model is shown to be converging. This rate of change is equally applied to all properties outlined above, except for Poisson's ratio. Additionally, to aid the convergence further the loading on the roof was applied in two stages. In the first stage, the self-weight, post-tensioning and the superimposed dead load are applied. Once this stage has converged, the live loading is applied and the workflow runs until it reaches a full solution. The full workflow is run on a virtual remote computer to maximise processing power and reduce analysis time.

### *4.2.5 Results*

Using the combination of the reduced safety factors and the advanced workflow and analysis described above, the team managed to justify the roof behaviour in line with the performance requirements. The outcome of the analysis shows a deflected shape which is heavily influenced by the deviations in the as-built shape of the roof. A significant amount of cracking and reductions in concrete stiffnesses were observed at the end of the analysis, but the roof deformation stabilises to the shape shown in Figure 10, with maximum deflections of no more than 30mm, showing that the roof does not exhibit snap through buckling failure. Therefore, the resistance to snap-through buckling is verified for the load case corresponding to the minimum reliability factor of $\beta = 3.3$.

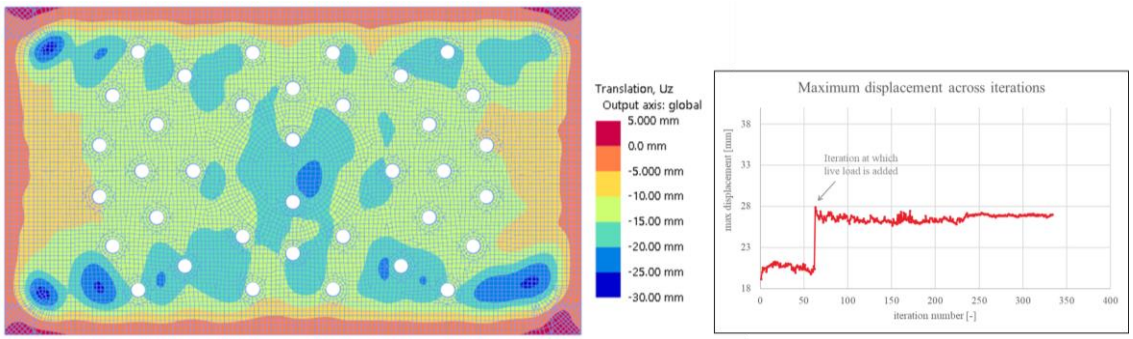


Figure 10 – Deflections across the roof at the end of the analysis (left) and across iterations (right)

## 5. Conclusion

The team was presented with the formidable challenge of re-justifying a historic structure which was not only at the forefront of engineering at the time it was designed but also appeared to deviate significantly from the design intent. By combining technical excellence, digital tools, and quantifying risk appropriately for an existing structure, it was demonstrated that the structure can meet the modern-day performance requirements without the need for any strengthening works. This shows the most sustainable outcome can be achieved to retain historic concrete shells of the past, allowing this beautiful 'thinner-than-an-eggshell' structure to continue its legacy.

Thanks to the outstanding work undertaken, the old finishes were removed, and the placing of the new finishes was completed with the final piece of copper laid in December 2023 by Chris Johnson, who worked as an apprentice with the original roofing team in the 1960s. Monitoring was carried out throughout the construction of the new finishes and showed the roof behaviour was as expected. The roof is now ready for the works inside the building to commence to turn the market hall into a museum.

Figure 11 - New copper finishes on the roof (taken March 2024) © FMJ Limited

## Acknowledgements

We would like to thank Ian Feltham, Dominic Munro, Steve McKechnie and Nuno Ferreira for embarking on this journey with us and providing their expertise in existing structures, concrete material, and advanced analysis; Joseph Cardoza for his commitment and dedication to the project; and Equans Regeneration Limited for their continued partnership and trust during the construction works.

## References

[1] P. Ahm and E. J. Perry, "Design of the Dome Shell Roof for Smithfield Poultry Market," *Proc. Instn civ. Engrs*, vol. 30, pp. 79-190, 1965.

[2] L. L. Jones and G. D. Base, "Test on a one-twelfth scale model of the dome shell roof for Smithfield Poultry Market," *Proc. Instn civ. Engrs*, vol. 30, pp. 79-130, 1965.

[3] Historic England, "Smithfield Poultry Market," July 2000. [Online]. Available: https://historicengland.org.uk/listing/the-list/list-entry/1381209. [Accessed March 2024].

[4] British Standards Institution, "BS EN 1990:2002+A1:2005 Eurocode - Basis of structural design," BSI, London, 2010.

[5] HM Government (United Kingdom), *The Building Regulations 2010 - Structure*, NBS, part of RIBA Enterprises Ltd, 2010.

[6] Fédération internationale du béton (fib), *fib Model Code for Concrete Structures 2010*, 2010.

[7] Fédération internationale du béton (fib), *fib Bulletin 80: Partial factor methods for existing concrete structures*, 2016.

[8] T. Vrouwenvelder and N. Scholten, "Assessment Criteria for Existing Structures," *Structural Engineering International*, Vols. Volume 20, 2010, no. Issue 1, pp. 62-65, 2018.